SOILS AND FOUNDATIONS Vol. 49, No. 2, 259–274, Apr. 2009
Japanese Geotechnical Society

AGING EFFECTS ON SMALL STRAIN SHEAR MODULI AND LIQUEFACTION PROPERTIES OF IN-SITU FROZEN AND RECONSTITUTED SANDY SOILS

TAKASHI KIYOTA[i], JUNICHI KOSEKI[ii], TAKESHI SATO[iii] and REIKO KUWANO[iv]

ABSTRACT

In order to investigate the effects of different geological ages on liquefaction properties of sandy deposits, a series of undrained cyclic triaxial tests was performed on three kinds of in-situ frozen and their reconstituted samples which were retrieved from Holocene (Tone-river sand) and Pleistocene (Edo-river B and C sands) deposits. The specimens were subjected to isotropic consolidation at a specified confining stress which is equivalent to the in-situ overburden stress at the depth of sampling, and small strain shear moduli were measured before and during the undrained cyclic loading tests. The liquefaction properties and the small strain shear moduli were affected by not only the natural aging effect of the specimen but also the inter-locking effect that was enhanced by applying drained cyclic loading before the undrained cyclic loading tests. During liquefaction, different tendencies of degradation in the small strain shear moduli which would reflect the aging effects of the specimen were observed between Tone-river Holocene sand and Edo-river B and C Pleistocene sands. The applicability of reconstituted samples as substitutes for in-situ frozen samples was confirmed with Tone-river Holocene sand that has no cementation effect between soil particles, whereas it seems difficult to simulate fully the liquefaction behaviour of Edo-river B and C Pleistocene sands which have higher cementation effect.

Key words: aging effect, in-situ frozen sample, liquefaction, sand, small strain characteristics (**IGC**: D6)

INTRODUCTION

Liquefaction resistance of a sandy soil deposit is influenced by not only relative density and the particle gradation including the fines content but also natural aging effect which affects the structure of soil particles. Since an old deposit may have strong aging effects, the Pleistocene sand deposits have not been considered as liquefiable in the relevant design guidelines in Japan. However, considering high values of the peak horizontal ground acceleration (PGA) recorded in recent large earthquakes in Japan (e.g., 818 gal during the 1995 Hyogo-ken Nanbu earthquake, 1676 gal during the 2004 Niigataken-Chuetsu earthquake and 879 gal during Niigataken-Chuetsu-oki earthquake), the liquefaction susceptibility of such Pleistocene deposits need to be re-evaluated (Yoshida et al., 2007).

In the laboratory tests, Yoshimi et al. (1984, 1994), Hatanaka et al. (1985) and Goto et al. (1992) showed that the liquefaction resistance of the in-situ frozen sample was significantly higher than that of the tube sample as well as a reconstituted sample. The difference in the liquefaction resistances of these samples was due to a disturbance of the tube sample and difference in the aging effects between the in-situ frozen sample and the other samples. Therefore, it has been considered that the use of the in-situ frozen sample is necessary to investigate the actual liquefaction behaviour, while it is costly.

In this study, the aging effects are considered to be developed by inter-locking and bonding (cementation) of the soil particles as reported by Barton (1993). Specifically, the inter-locking between soil particles is structured due to change in the environment; for example, creep deformation with time, earthquake histories and change in the effective overburden pressure due to change in the water table or the land form. Moreover, as time passes by, the bonding effects may have taken place due to the chemical reaction. In the previous study that focused on the bonding effect, Koseki and Ohta (2001) investigated the effects of different consolidation conditions on liquefaction characteristics of artificial samples prepared by mixing Toyoura sand and bentonite clay. In addition, the increase in the liquefaction resistance due to application of drained cyclic loading before liquefaction tests has been observed, since the inter-locking between the soil particles would be enhanced by such a loading history

i) Assistant Professor, Tokyo University of Science, Japan (kiyo@rs.noda.tus.ac.jp).
ii) Professor, Institute of Industrial Science, University of Tokyo, Japan.
iii) Research Support Promotion Member, ditto.
iv) Associate Professor, ditto.
The manuscript for this paper was received for review on July 28, 2008; approved on January 5, 2009.
Written discussions on this paper should be submitted before November 1, 2009 to the Japanese Geotechnical Society, 4-38-2, Sengoku, Bunkyo-ku, Tokyo 112-0011, Japan. Upon request the closing date may be extended one month.

(Yoshimi et al., 1994). The liquefaction resistance, which is affected by the aging effect due to natural or artificial processes, has been studied, focusing on its possible correlation with small strain characteristics by Tokimatsu and Hosaka (1986) and Teachavorasinskun et al. (1994) among others.

The small strain characteristics that are measured with strain level of less than 10^{-5}, such as shear modulus or Young's modulus are one of the important parameters which reflect the current soil structure including the aging effects. Tanizawa et al. (1994), Goto et al. (1999) and Zhou and Chen (2005) showed degradation of the small strain shear moduli of sands that were measured dynamically during undrained cyclic triaxial tests. Koseki et al. (2000) compared the small strain characteristics of Toyoura sand that were measured statically during isotropic consolidation and liquefaction process, and summarized that the values of small strain moduli during liquefaction are smaller than those during isotropic consolidation because of damage to soil structure due to liquefaction. However, as far as authors are aware, there have been few studies that deal with the liquefaction behaviour of in-situ frozen specimens which have different aging effects, in particular with small strain characteristics.

In this study, therefore, in order to investigate the relationships between aging effects, liquefaction behaviour and small strain characteristics, a series of undrained cyclic triaxial tests was performed on high quality in-situ frozen samples from Holocene and Pleistocene deposits, and their reconstituted samples. The degradation of the aging effects of each sample on the liquefaction behaviour was investigated based on the small strain characteristics. In addition, the applicability of reconstituted samples as substitutes for in-situ frozen samples was discussed based on the concept that the liquefaction resistance of a disturbed sample would be the same as that of an undisturbed sample when their relative densities and small strain characteristics are adjusted as proposed by Tokimatsu and Hosaka (1986).

TESTED MATERIALS

Three kinds of in-situ frozen samples (denoted as FSs) tested in this study were taken from a Holocene deposit (denoted as Tone-river sand) and Pleistocene deposits (denoted as Edo-river B and C sands). They are sandy soils, and their fines contents are less than 3% as summarized in Table 1. The geological ages of these deposits were older in the order of the Edo-river C sand, the Edo-river B sand, and the Tone-river sand (Kiyota et al., 2009). In addition, reconstituted samples were also used in this study. The details of their preparation procedures are shown later.

TEST APPARATUS

An automated triaxial apparatus was used to test cylindrical specimens that were approximately 50 mm in diameter and 100 mm in height. Refer to Kiyota et al. (2009) for the details of the apparatus and the transducers employed. The vertical static Young's modulus, E_v, was evaluated from the small cyclic stress-strain relationships with a double amplitude vertical strain of approximately 0.002%, which were measured with a pair of local deformation transducers (LDTs, Goto et al., 1991). To calculate the static shear moduli, G_s^* (denoted as G_s), from the E_v, Eq. (1) was used while considering the effects of inherent and stress-induced anisotropies on the small strain properties (Tatsuoka, et al., 1999).

$$G_s=\frac{E_v}{2(1+\nu_0)}\cdot\frac{2(1-\nu_0)}{1+a\cdot R^n-2\sqrt{a}\cdot R^{n/2}\cdot\nu_0} \tag{1}$$

where R is the principal stress ratio ($=\sigma_v'/\sigma_h'$), a is the parameter regarding the inherent anisotropy of Young's moduli, and n is the power number that is related with the stress-state dependency of Young's moduli. Note that the value of the reference Poisson's ratio, ν_0, was set to be 0.17, which was assumed for the fine sand based on the study by Hoque and Tatsuoka (1998).

Since the static Young's moduli of saturated specimens obtained under undrained condition are affected by change in the pore water pressure during small cyclic loading and inherent and stress-induced anisotropies, the values of E_v during liquefaction were converted to those under drained condition by Tatsuoka et al. (1997) as:

$$E_v=E_{vu}\frac{1+2(aR^n)^{0.5}\nu_0 x}{1+x} \tag{2}$$

where x is the stress increment ratio during small cyclic vertical loading under undrained condition given by:

Table 1. Basic properties of testes samples (after Kiyota et al., 2009)

Sample	Depth (GL-m)	σ_z'* (kPa)	D_{50} (mm)	F_c (%)	U_c	e_{max}	e_{min}	V_s** (m/s)	*Geological age*
Tone-river	11.8 ~ 12.1	100	0.188	1.2	2.0	1.066	0.675	240	Holocene deposit (8,000 yr)
Edo-river B	10.3 ~ 11.0	100	0.561	3.0	4.3	1.043	0.710	270	Young Pleistocene deposit ($130*10^3$ yr)
Edo-river C	16.0 ~ 16.3	160	0.189	2.9	2.1	1.132	0.714	390	Old Pleistocene deposit ($130*10^3$ ~ $300*10^3$ yr)

*σ_z' is in-situ overburden stress at the depth of sampling
**V_s is shear wave velocity measured by in-situ PS logging

$$x=-\left(\frac{d\sigma'_h}{d\sigma'_v}\right)=\frac{1-2(aR^n)^{0.5}\nu_0}{2aR^n[1-\nu_0-(aR^n)^{-0.5}\nu_0+2(bE_h/\sigma'_h d)]} \quad (3)$$

where E_{vu} is vertical Young's moduli under undrained condition, E_h is horizontal Young's moduli under drained condition that are formulated as a function of the current effective horizontal stress σ'_h, and d is the diameter of the specimen in cm. Note that the parameter regarding the effects of membrane penetration, b, was set to $1.7\times10^{-3}/\ln 10$, which was experimentally obtained by Goto (1986) for fine sand. The value of a was back-calculated with Eqs. (2) and (3) from the E_{vu} and E_v values which were measured during isotropic consolidation. As a result, the a value was set at 1.2 for reconstituted sample of the Edo-river B sand, and 0.8 for the other samples. Note that the a value is the inherent anisotropy parameter represented as E_v/E_h. Hoque and Tatsuoka (1998) reported some degree of inherent anisotropy with $E_v>E_h$ for Toyoura sand, which corresponds to the result of the reconstituted sample of the Edo-river B sand. This feature is opposite to that of $E_v>E_h$ by AnhDan and Koseki (2003), which corresponds to the other samples in this study. Although the specific reasons are not known to the authors, the type of the samples (FS and reconstituted sample) as well as the difference in the uniformity coefficient, U_c, between the Edo-river B sand and the other samples (*see* Table 1) could influence the value of a. The value of n was obtained by using Eq. (4) (Tatsuoka and Kohata, 1995). In this study, different values of n were set for respective specimens based on the results from measurements of E_v during isotropic consolidation.

$$E_v=E_{v0}\cdot\left(\frac{\sigma'_v}{\sigma'_{v0}}\right)^n \quad (4)$$

where E_{v0} is the value of E_v when σ'_v is equal to a reference pressure, σ'_{v0} (100 kPa in this study).

As small strain characteristics, the dynamic shear modulus, G_d, was also measured in this study. A pair of accelerometers was used to measure the arrival of S wave at two different heights on the side surface of the specimen and thus evaluate the dynamic shear moduli employing the following equation. Refer to Kiyota et al. (2009) as well for the details of the dynamic measurement.

$$G_d=\rho\cdot V_s^2 \quad (5)$$

where ρ is the mass density of the specimen, and V_s is S wave velocity.

TEST PROCEDURES

In this study, since a low confining pressure during thaw process caused disturbance to the FSs as reported by Kiyota et al. (2009), the FSs were thawed at a confining pressure of 98 kPa which is almost equivalent to the in-situ overburden stress at the depth of sampling of the Tone-river sand and the Edo-river B sand (*see* Table 1) as well as the limit value of the capacity of conventional vacuum pumps. On the other hand, the FSs of Edo-river C sand were thawed at confining pressure of 30 kPa or 98 kPa which is lower than those of in-situ overburden stress. However, Kiyota et al. (2009) confirmed that the disturbance due to low confining pressure with Edo-river C sand was insignificant. The other details of the sample preparations were given elsewhere (Kiyota et al., 2009). The FSs were saturated while keeping a constant confining pressure. After confirming that the B value of the specimens is not smaller than 0.96, the specimens were subjected to isotropic consolidation up to a specified confining stress which is equivalent to the in-situ overburden stresses at the depth of sampling, with a back pressure of 200 kPa.

· The reconstituted samples (denoted as RSs) of the above three samples were prepared in order to study the effect of aging. The RSs were prepared by pluviating oven-dried material of the FSs through air, and the height of pluviation was changed to adjust the dry densities at the same level as that of the FS. After saturating at a confining pressure of 30 kPa and confirming the B value of the specimen ($B>0.96$), the RSs were consolidated to the same isotropic effective stress states as those of respective FSs with a back pressure of 200 kPa. After isotropic consolidation, some of the RSs were subjected to 10,000 or 20,000 cycles of vertical load with double amplitude vertical strain, $\varepsilon_{v(DA)}$, of 0.1% at $\dot{\varepsilon}_v=0.6\%$/min under drained condition. This is one of the procedures to increase the stiffness and the liquefaction strength of the specimen without significantly changing the specimen density (Drnevich and Richart, 1970; Seed, 1979), and Goto (1993) also used the value of $\varepsilon_{v(DA)}$ of 0.1% to increase the liquefaction resistance. The RS which has such a stress history is called RSCL in this paper.

After the above procedures, undrained cyclic triaxial tests were performed with constant amplitude of cyclic stress at $\dot{\varepsilon}_v=0.2\%$/min. The static and dynamic small strain shear moduli, G_s^* and G_d, were measured on the FSs, RSs and RSCLs during the processes of the isotropic consolidation and the undrained cyclic loading. When the G_s^* and G_d were measured during undrained cyclic loading, the $\dot{\varepsilon}_v$ value was reduced to 0.02%/min.

TEST RESULTS

Small Strain Characteristics during Isotropic Consolidation

In order to normalize for the effects of different void ratios, e, the following function proposed by Hardin and Richart (1963) is applied to normalize the shear moduli measured by static and dynamic measurement, G_s^* and G_d.

$$f(e)=(2.17-e)^2/(1+e) \quad (6)$$

Figure 1 shows the relationships between G_s^*, G_d and a stress parameter, $(\sigma'_v\cdot\sigma'_h)^{0.5}$, of the Tone-river sand measured during isotropic consolidation. The G_s^* and G_d values for the FSs were measured only at $\sigma'_v=\sigma'_h=100$ kPa because the initial isotropic stress state of the FSs was 98 kPa. Data with small dots and thin lines represent the test results of individual specimens of the FSs and the

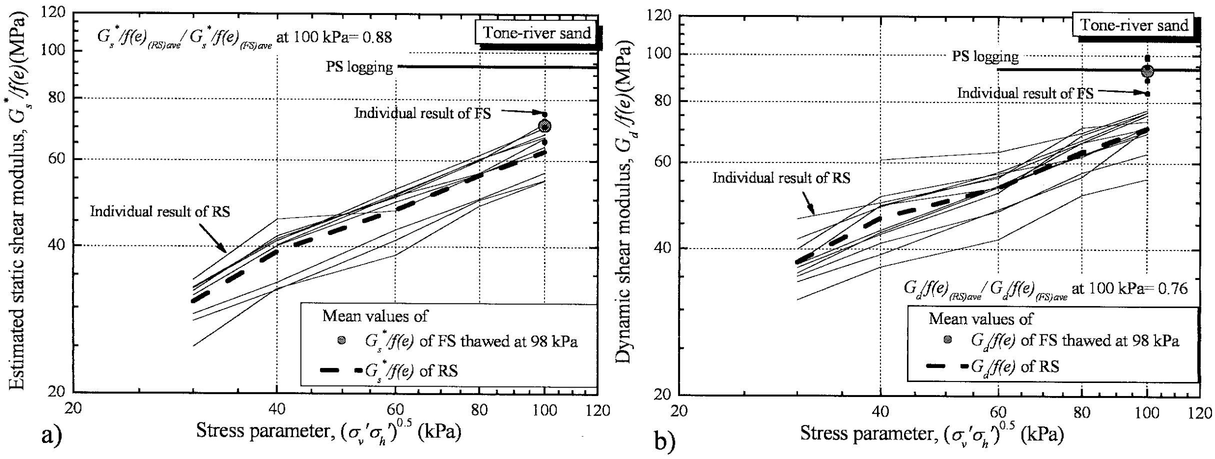

Fig. 1. Relationships between a) $G_s^*/f(e)$ and $(\sigma_v'\sigma_h')^{0.5}$, and b) $G_d/f(e)$ and $(\sigma_v'\sigma_h')^{0.5}$ of Tone-river sand

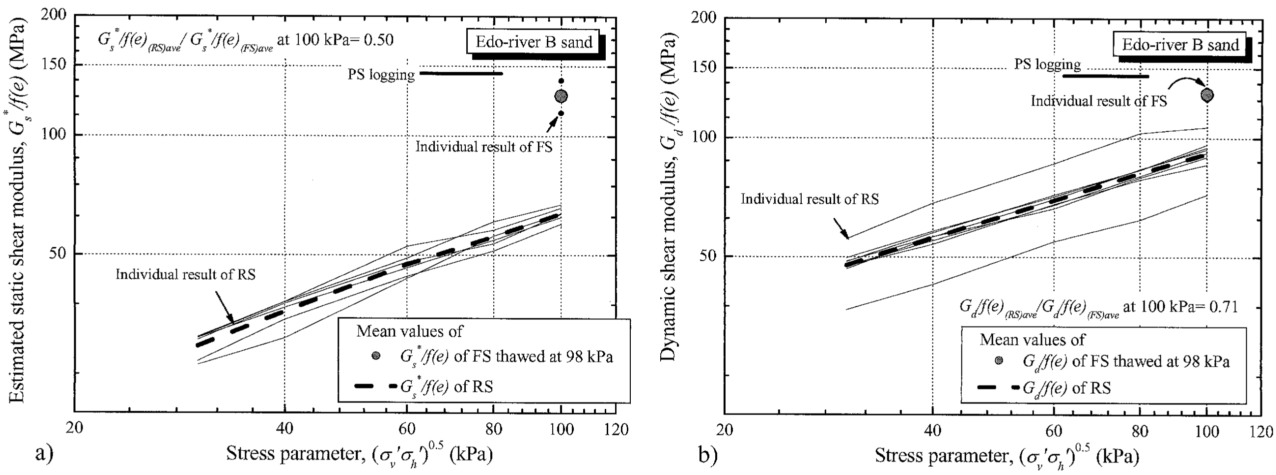

Fig. 2. Relationships between a) $G_s^*/f(e)$ and $(\sigma_v'\sigma_h')^{0.5}$, and b) $G_d/f(e)$ and $(\sigma_v'\sigma_h')^{0.5}$ of Edo-river B sand

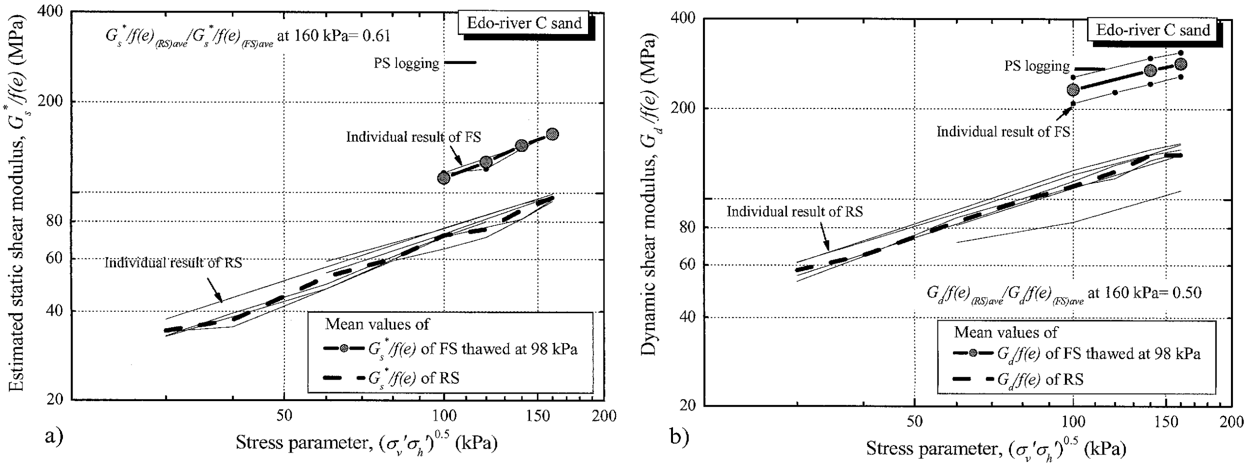

Fig. 3. Relationships between a) $G_s^*/f(e)$ and $(\sigma_v'\sigma_h')^{0.5}$, and b) $G_d/f(e)$ and $(\sigma_v'\sigma_h')^{0.5}$ of Edo-river C sand

RSs, respectively. Meanwhile, data with a circle symbol and a thick broken line represent the average values of test results on the FSs and the RSs, respectively. The G_s^* and G_d values increased with increase in the stress level, and their average values for the FSs were larger than those for the RSs even though they were normalized by the void ratio function of Eq. (6).

Figures 2 and 3 show the G_s^* and G_d values of the Edo-river B and C sands measured during isotropic consolidation. Note again that the G_s^* and G_d values for the FSs were measured at a confining pressure of 100 kPa because the initial isotropic stress state of the FSs was 98 kPa. The average values of G_s^* and G_d for the FSs were larger than those of the RSs.

The results of in-situ PS logging are also shown in Figs. 1, 2 and 3 with thick horizontal lines. The range of the horizontal line represents the in-situ stress states (estimated assuming $\sigma'_h/\sigma'_v=0.5$) of the soil layer where the FSs were retrieved. Since the G_d values of the FSs were almost similar to the results of in-situ PS logging as shown in Figs. 1(b), 2(b) and 3(b), it could be inferred that the disturbance of the FSs was small. However, the G_s^* values were smaller than the G_d values. Such a feature that small strain moduli by dynamic measurement are larger than those by static measurement has been reported by previous researches (e.g., Yamashita, et al., 2003). In particular, Tanaka et al. (1994) showed that the stiffness from the static measurement refers to the overall deformation behaviour, whereas the elastic wave measurement reflects predominantly that of the local stiff part.

The remarkable feature of the test results shown in Figs. 1 to 3 was the difference in the shear moduli between the FSs and the RSs. The ratios of average value of G_s^* and G_d of the RSs to those of the FSs, $G^*_{s(RS)ave}/G^*_{s(FS)ave}$ and $G_{d(RS)ave}/G_{d(FS)ave}$, which were measured at the end of isotropic consolidation are also shown in these figures. Since it would be reasonable to assume that the FSs from both the Holocene and the Pleistocene deposits have their own aging effects while their RSs do not have such effects, the values of $G^*_{s(RS)ave}/G^*_{s(FS)ave}$ and $G_{d(RS)ave}/G_{d(FS)ave}$ reflect probably the degree of aging effects of each deposit.

Note again that the aging effects in this study are considered to be developed by inter-locking and cementation. Especially, in the case of Pleistocene deposits like the FSs of Edo-river B and C sands, the cementation effect may have taken place due to the diagenesis.

Kiyota et al. (2009) performed unconfined compression tests on the same materials as tested in this study. As summarized in Table 2, the cementation effect of Edo-river C sand could be stronger than that of Edo-river B sand, and Tone-river sand and the RSCL are not influenced by this factor. Therefore, the larger values of the small strain shear moduli with the FS of Tone-river sand in comparison with the RSs (*see* Fig. 1 and Table 2) would not be due to cementation but due to inter-locking of soil particles.

Possible Aging Effects due to Cyclic Loading History

Drnevich and Richart (1970) showed that the stiffness of the specimen is increased due to cyclic loading history without significant volume change of the specimen. On the other hand, Wichtmann and Triantafyllidis (2004) showed only moderate changes of small strain stiffness even though 100,000 cycles of vertical loading was applied. Those previous studies were carried out with dry sands while saturated sands were used in the present study. In any case, if the aging effects of specimen could be linked with the small strain characteristics as mentioned above, they would be more or less produced by drained cyclic loading history. In this study, some of the RSs were subjected to 10,000 or 20,000 cycles of vertical loading with constant $\varepsilon_{v(DA)}$ of 0.1% under drained condition after isotropic consolidation.

Figure 4 shows the relationships between number of cycles and changes in the shear moduli of all samples. The increases in the static and dynamic shear moduli, G_s^* and G_d, were observed with increase in the number of cycles. This feature implies that the specimen could be strengthened with enhanced inter-locking between the soil particles due to drained cyclic loading. Seed (1979) and

Table 2. Small strain shear moduli, liquefaction resistance and unconfined compression strength of tested samples

Sample	Type	$G^*_{s\,ave}/f(e)^+$ (MPa)	$G_{d\,ave}/f(e)^+$ (MPa)	R_{L15}	Reduction rate for G_s^{*++}	Reduction rate for G_d^{++}	Reduction rate for R_{L15}^{++}	q_u^{+++} (kPa)
Tone-river	FS	70.8	93.1	0.43	—	—	—	Liquefied
	RS	62.6	70.7	0.17	12%	24%	60%	—
	$RSCL_{(10000)}$	75.6	91.6	0.43	△7%	2%	0%	—
Edo-river B	FS	126.3	129.1	0.40	—	—	—	19.5
	RS	63.7	91.5	0.16	50%	29%	60%	—
	$RSCL_{(20000)}$	82.8	115.3	0.38	34%	11%	5%	—
Edo-river C	FS	157.4	283.7	0.32	—	—	—	28.6
	RS	96.5	140.7	0.14	39%	50%	57%	—
	$RSCL_{(20000)}$	132.3	192.3	0.30	16%	32%	6%	Liquefied

+: Average values of $G_s^*/f(e)$ and $G_d/f(e)$ measured immediately before the liquefaction test ($\sigma'_v=\sigma'_h=100$ kPa for Tone-river sand and Edo-river B sand: $\sigma'_v=\sigma'_h=160$ kPa for Edo-river C sand)

++: Defined, for example, as $\left\{1-\dfrac{G^*_{s(RS)ave}}{G^*_{s(FS)ave}}\right\}\times 100$ (%), for the case with G_s^* of RS

+++: Refer to Kiyota et al. (2009)

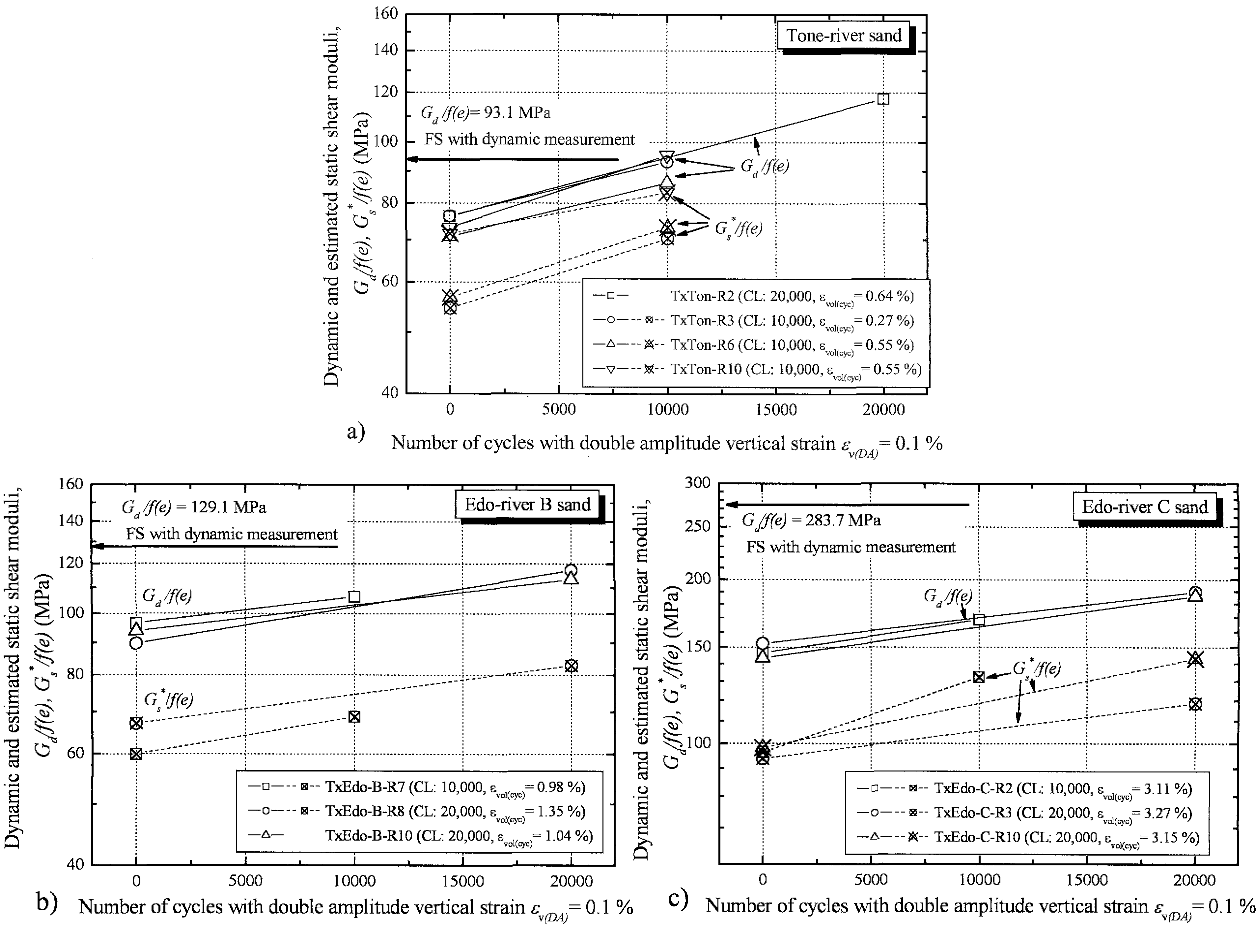

Fig. 4. Relationships between number of drained cycles and small strain shear moduli of a) Tone-river sand, b) Edo-river B sand and c) Edo-river C sand

Tokimatsu and Hosaka (1986) among others reported that such drained small cyclic loading caused increase in stiffness as well as liquefaction resistance of the specimen. The change in the liquefaction resistance is shown later.

The G_d values of the RSs after drained small cyclic loading became similar to or larger than that of the FS in the case of Tone-river sand as shown in Fig. 4(a). Therefore, the RSs of Tone-river sand seem to have produced the same aging effect as the FSs in terms of the small strain shear moduli. On the other hand, as shown in Figs. 4(b) and (c), the G_d values of the RSs of Edo-river B and C sands could not reach the G_d values of the FSs even though the number of cycles exceeded 20,000.

The shear moduli could be also increased due to a densification of the specimens by drained cyclic loading. As shown in Fig. 4, the increment in the volumetric strain caused by drained cyclic loading, $\varepsilon_{vol(cyc)}$ was approximately 0.5%, 1% and 3% for Tone-river sand, Edo-river B sand and Edo-river C sand, respectively. However, since the values of shear moduli were increased by the application of the drained cyclic loading even though they were normalized by the void ratio function, such increment in the shear moduli could be linked with enhanced interlocking between the soil particles.

Liquefaction Properties

Figures 5 and 6 show the typical results of undrained cyclic triaxial tests on a FS of the Tone-river sand and its RS respectively. The square symbols on the stress-paths and stress-strain relations represent the measuring points of small strain shear moduli, G_s^* and G_d. As shown in the figures, the respective relative densities, D_r, of the FS and the RS were similar to each other.

However, as indicated on the stress-paths shown in Figs. 5(a) and 6(a), the liquefaction processes of the FS and the RS were different from each other irrespective of the same cyclic stress ratios applied, $\sigma_d/2\sigma_c'=0.4$ where σ_d and σ_c' denote single amplitude of the cyclic vertical stress and the effective confining pressure at the end of isotropic consolidation, respectively. The effective stress of the RS was decreased significantly at the first cycle (Fig. 6(a)), whereas that of the FS was decreased gradually with the increase in the number of cycles as shown in Fig. 5(a).

As indicated on the stress-strain relations shown in Figs. 5(b) and 6(b), developments of the ε_v which shifted to the extension side could be observed with both the FS and the RS. The increase in the $\varepsilon_{v(DA)}$ with the number of cycles, N_c, of the RS was more significant than that of the FS. More specifically, the required numbers of cycles to cause $\varepsilon_{v(DA)}=3\%$ of the FS and the RS which are shown in

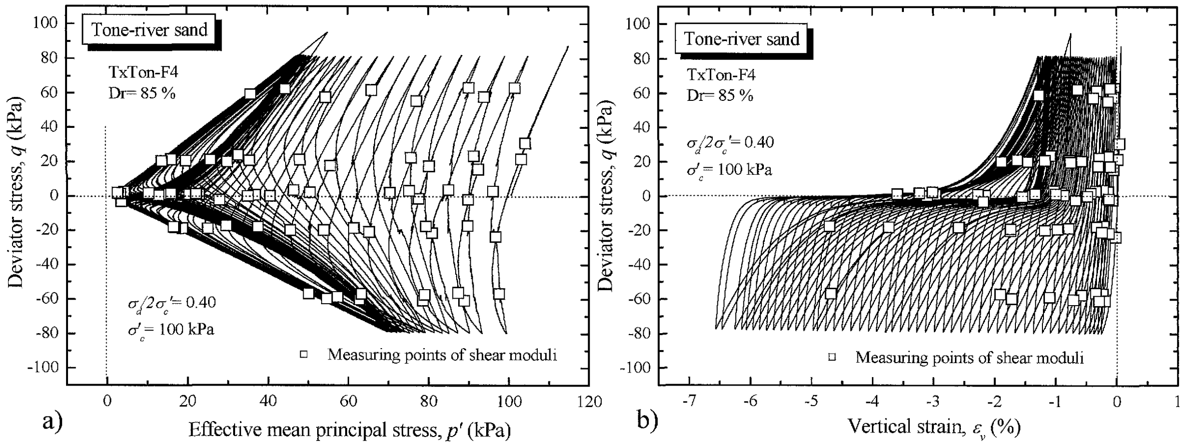

Fig. 5. a) Effective stress path and b) stress-strain relation during liquefaction test of FS of Tone-river sand

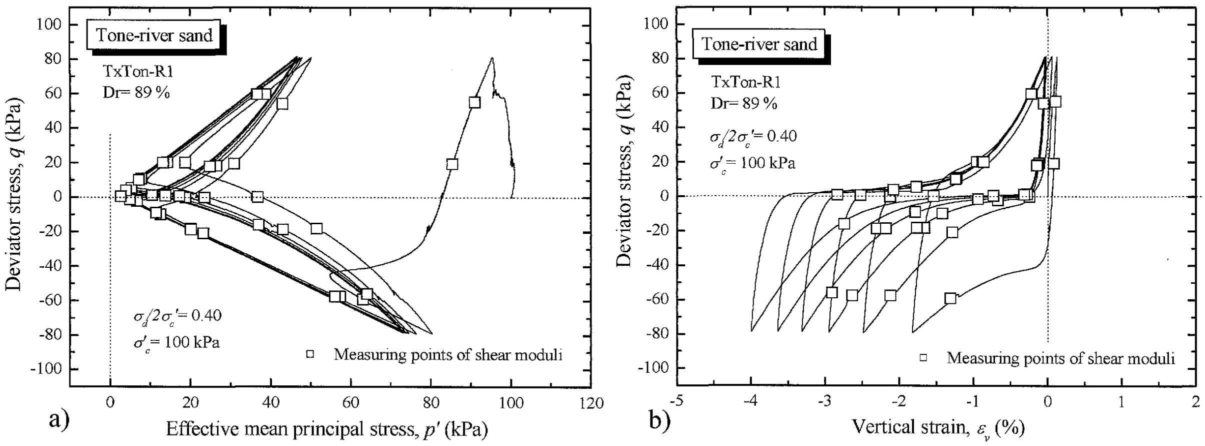

Fig. 6. a) Effective stress path and b) stress-strain relation during liquefaction test of RS of Tone-river sand

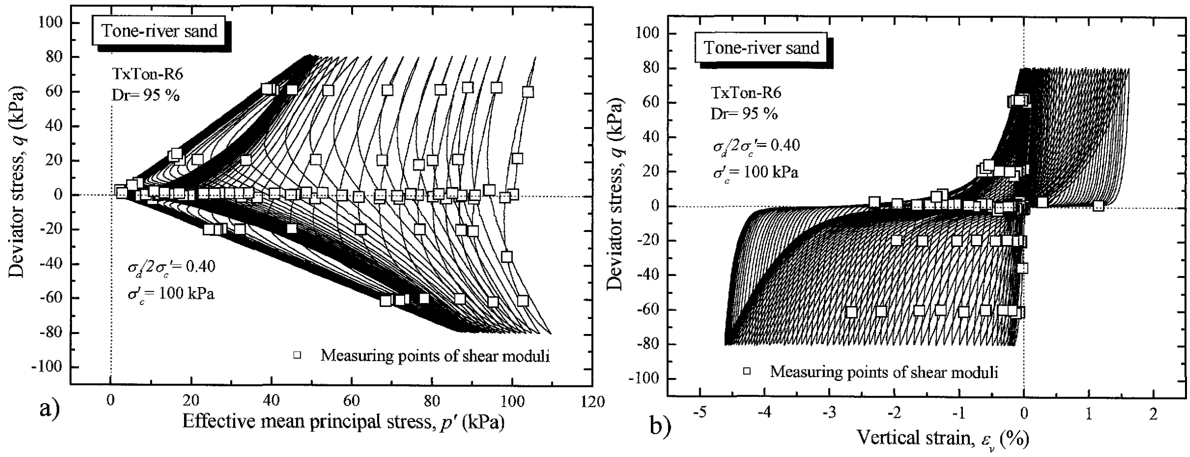

Fig. 7. a) Effective stress path and b) stress-strain relation during liquefaction test of RSCL of Tone-river sand

Figs. 5 and 6, were 29 and 3.5, respectively.

Figure 7 shows the undrained cyclic test results of a RSCL of the Tone-river sand which was subjected to 10,000 cycles of vertical load with $\varepsilon_{v(DA)} = 0.1\%$ under drained condition after isotropic consolidation. The liquefaction behaviour of the RSCL was totally different from that of the RS (Fig. 6). The extent of the reduction of effective stress of the RSCL was much smaller than that of the RS. Although the relative density, D_r, of the RSCL was higher than those of the FS and the RS, the liquefaction behaviour of the RSCL rather corresponded to that of the FS (Fig. 5). It could be inferred that the higher liquefaction resistance of the RSCL was caused by formation of inter-locking of the soil particle due to the application of drained cyclic loading before the liquefaction test as mentioned previously. However, as indicated on the stress-strain relation shown in Fig. 7(b), development of the ε_v values to both the compression and the extension sides could be observed with the RSCL, while they shifted only to the extension side for the FS (Fig. 5(b)). Figure 8 shows the stress-strain relations of the RSCL for the first and 10,000th cycles during the drained cyclic loading with constant $\varepsilon_{v(DA)}$ of 0.1%. The stress-strain relation after the 10,000 cyclic loading shifted by about 20 kPa to the extension side. This anisotropic stress history of the RSCL could probably cause the different stress-strain behavior from the FS. On the other hand, for the RSCL (Fig. 7(b)), since the ε_v values shifted to the compression side when $\varepsilon_{v(DA)}$ exceeded about 4.5%, there is a possibility that a strain localization was developed, which altered the overall deformation characteristics as well.

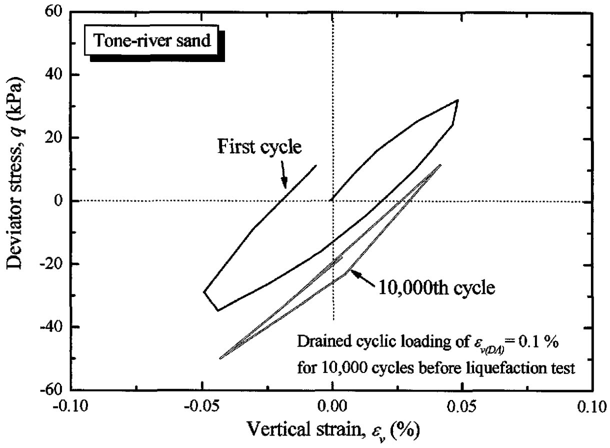

Fig. 8. Stress-strain relations during drained cyclic loading of RSCL of Tone-river sand

Other series of undrained cyclic triaxial tests were performed with Edo-river B and C sands. As shown in Figs. 9(a), (b), 10(a) and (b), the tendency of the reduction of effective stress for the FSs and the RSs of Edo-river B and C sands were similar to that of the Tone-river sand shown in Figs. 5(a) and 6(a), even though the relative density of the RS of Edo-river C sand was higher than that of the FS. In addition, the liquefaction resistance of the RSCL of Edo-river B and C sands became larger than that of the RS due to the application of 20,000 cyclic loading with $\varepsilon_{v(DA)}$ of 0.1% under drained condition as shown in Figs. 9(b), (c), 10(b) and (c). However, the liquefaction resistance of the RSCL seems to be still lower than that of the FS for Edo-river C sand. It was also the case with Edo-river B sand, although the difference in the liquefaction resistance of the RSCL and the FS became

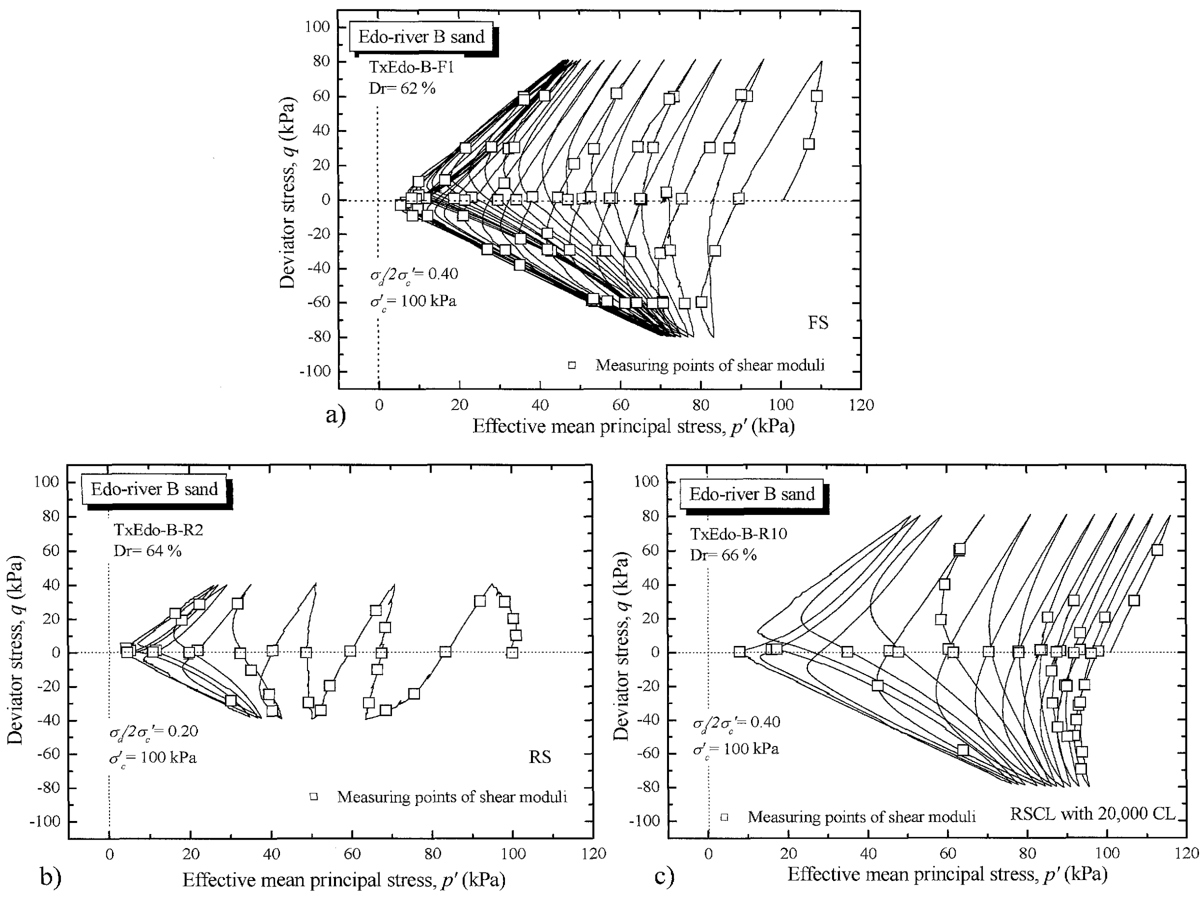

Fig. 9. Effective stress paths of a) FS, b) RS and c) RSCL of Edo-river B sand

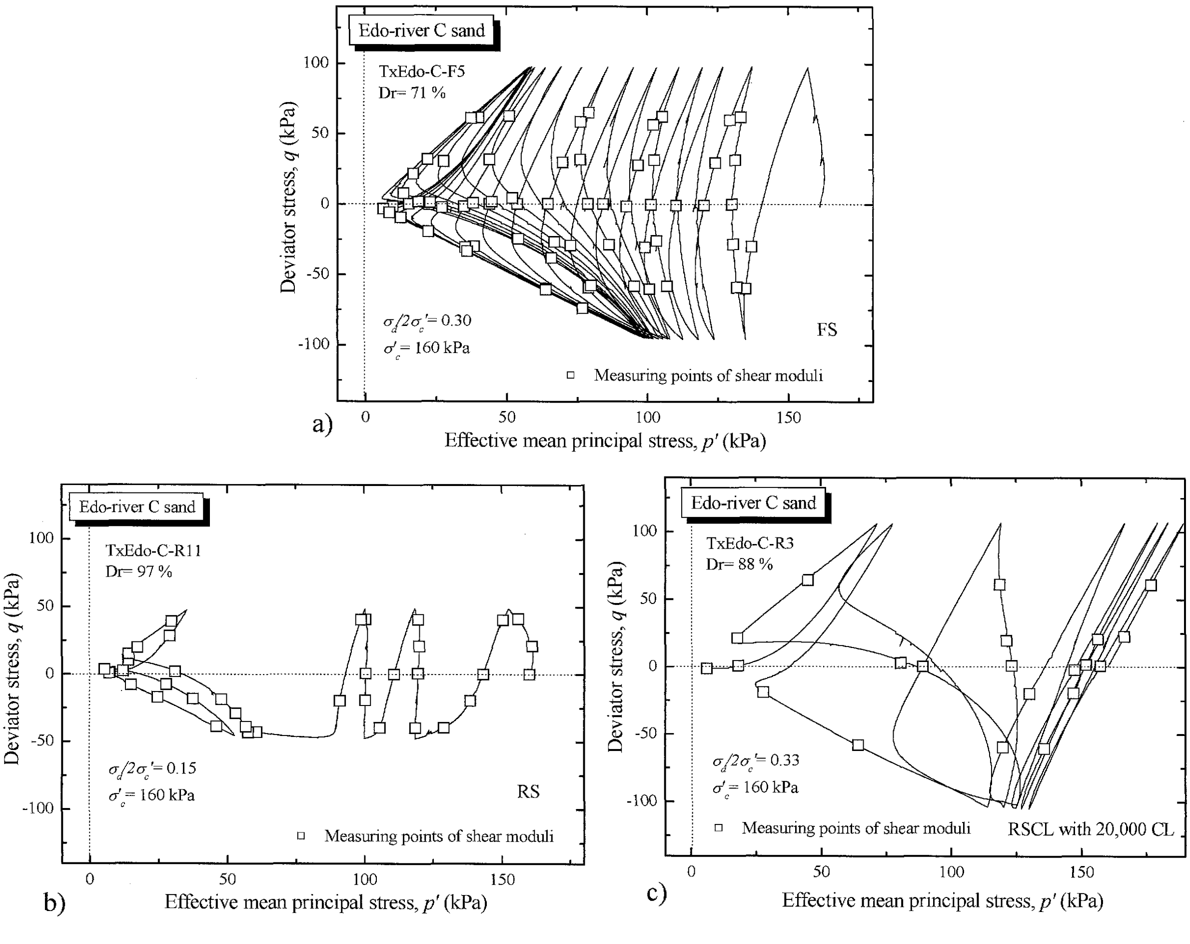

Fig. 10. Effective stress paths of a) FS, b) RS and c) RSCL of Edo-river C sand

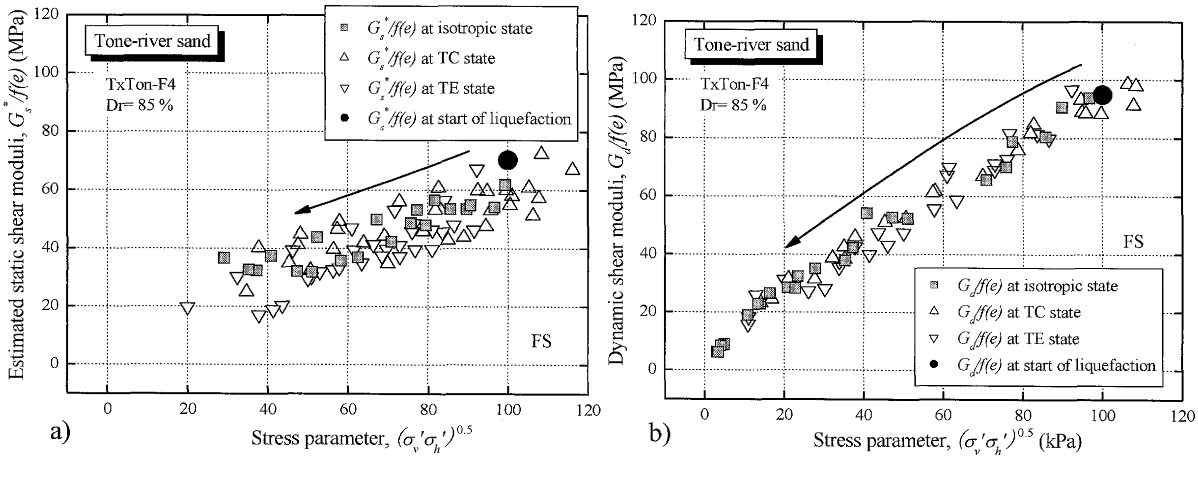

Fig. 11. a) $G_s^*/f(e)$ and b) $G_d/f(e)$ during liquefaction process of FS of Tone-river sand

smaller. Since, they were similar to each other for Tone-river sand, it could be suggested that the aging effects of the FSs were stronger in the order of Edo-river C sand, Edo-river B sand and Tone-river sand.

Figure 11 shows the values of G_s^* and G_d of the FS of Tone-river sand during undrained cyclic triaxial test, which were measured under the isotropic state, triaxial compression (denoted as TC) state and triaxial extension (denoted as TE) state, and plotted versus the effective stress parameter, $(\sigma_v' \cdot \sigma_h')^{0.5}$. Decrease in the values of G_s^* and G_d was observed with the decrease in $(\sigma_v' \cdot \sigma_h')^{0.5}$ during liquefaction. However, the G_s^* values somewhat fluctuated while more unique relationships between G_d and $(\sigma_v' \cdot \sigma_h')^{0.5}$ could be observed. Figure 12 shows the G_d values of the RS and the RSCL of Tone-river sand. Although their initial values were different from that of the FS, they exhibited a trend of reduction during liquefaction that was similar to that with the FS as shown in

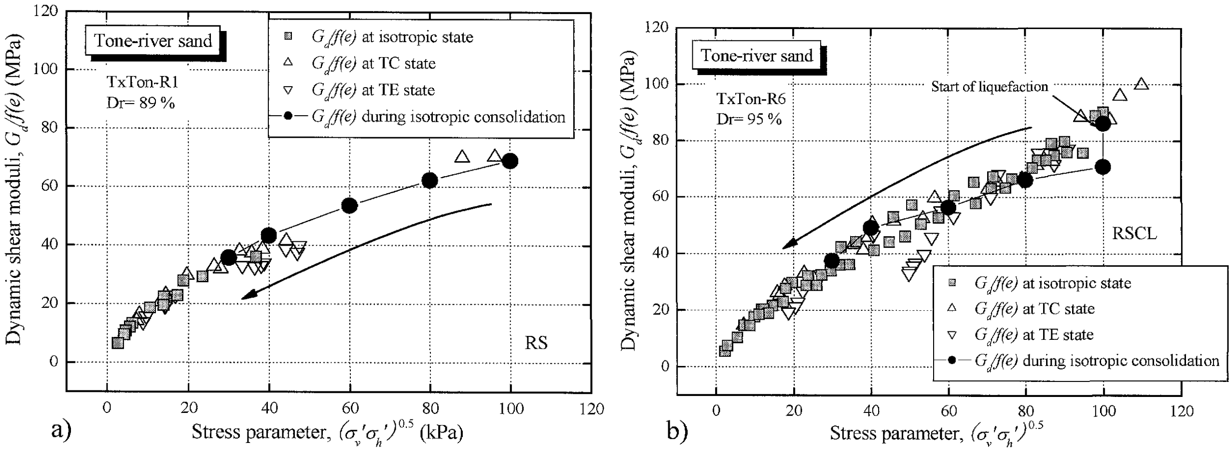

Fig. 12. $G_d/f(e)$ during liquefaction process of a) RS and b) RSCL of Tone-river sand

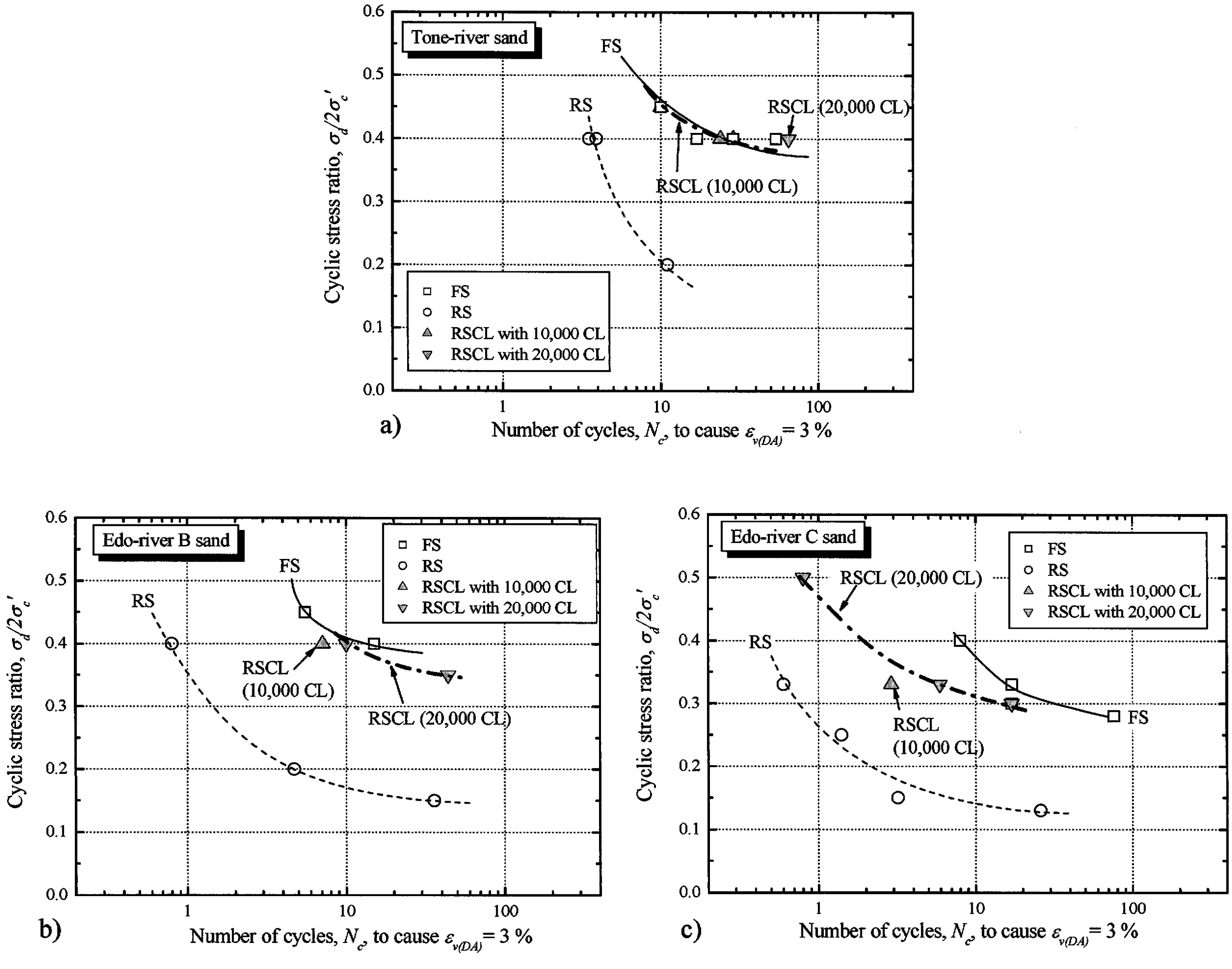

Fig. 13. Liquefaction resistance curves between $\sigma_d/2\sigma_c'$-N_c of FS, RS and RSCL from a) Tone-river sand, b) Edo-river B sand and c) Edo-river C sand

Fig. 11(b). With the RS, the G_d values during liquefaction were equal to or slightly smaller than those during isotropic consolidation under the same stress level. This may suggest that soil structure was less stable during liquefaction than during isotropic consolidation. Further discussion on the small strain shear moduli during liquefaction are given later.

Figure 13 compares the relationships between the cyclic stress ratio, $\sigma_d/2\sigma_c'$, and the number of cycles required to cause $\varepsilon_{v(DA)}=3\%$ for all samples. The resistances of the FSs against liquefaction were obviously higher than those of the RSs for all samples. Hatanaka et al. (1985) and many studies have reported the same tendency as obtained in this study. It should be noted again that the liquefaction resistances of the RSCLs were increased significantly and approached those of the FSs. Note also that the extent of the increase in the liquefaction resistance of the RSCLs seem to be linked with the number of drained cyclic loading.

The reduction rate for the liquefaction resistance defined as the $\sigma_d/2\sigma'_c$ to cause $\varepsilon_{v(DA)}=3\%$ in 15 cycles, R_{L15}, were shown in Table 2. The reduction rate for the R_{L15} of the RSs of the Edo-river B and C sands should be higher than that of the Tone-river sand if the aging effects of the former sands are stronger than those of the latter sand. However, in the present study, the differences in the values of reduction rate for the R_{L15} between the Holocene and the Pleistocene sands were relatively small in comparison with the differences in those for G_s^* and G_d that were measured during isotropic consolidation as shown in Figs. 1, 2 and 3.

Correlations between Liquefaction Resistance and Small Strain Characteristics

Figure 14 shows the relationships between the R_{L15} and small strain shear moduli, G_{sN}^* and G_{dN}, which were measured immediately before the liquefaction tests. The values of G_{sN}^* and G_{dN} were evaluated by the following equation in order to normalize for the effects of minimum void ratio, e_{min}, and the stress level, as proposed by Tokimatsu and Uchida (1990).

$$G_N=\frac{G}{f(e_{min})}\cdot\left(\frac{\sigma'_0}{\sigma'_m}\right)^n \tag{7}$$

where σ'_0 is reference pressure (100 kPa in this study), σ'_m is the effective stress (denote as $(\sigma'_v\cdot\sigma'_h)^{0.5}$) when the shear moduli (G_s^* or G_d) were measured and $f(e_{min})$ is the value of the void ratio function (Eq. (6)) at the minimum void ratio. Note that the power number, n, is the same as used in Eq. (1).

As shown in Fig. 14(a), relationships between the values of G_{dN} and R_{L15} were unique for each sample, while they were different from each other, depending on the types of the tested material. A larger value of R_{L15} was observed when G_{dN} was larger. In the case of the RSCL of Tone-river sand with 10,000 cycles, almost the same values of G_{dN} and R_{L15} were obtained as those of the FS. In the case of Edo-river B and C sands, although the values of G_{dN} and R_{L15} of the RSCL could not reach those of the FS, they were significantly increased from the original values of the RS.

Note again that the unconfined compression tests could not be carried out with the FS of Tone-river sand and the RSCL of Edo-river C sand as summarized in Table 2. This observation suggests that the larger values of the small strain shear moduli and liquefaction resistance with the FS of Tone-river sand and the RSCL in comparison with the RSs (*see* Figs. 13 and 14) would not be due to cementation but due to inter-locking of soil particles.

Meanwhile, the relationships between the G_{sN}^* and the R_{L15} shown in Fig. 14(b) rather fluctuated in comparison with the G_{dN} and R_{L15} relations. In this study, therefore, the small strain shear moduli by dynamic measurement, G_d, was found to be more relevant than those by static measurement, G_s^*, in estimating the liquefaction resistance, which is affected by the aging effects.

DISCUSSIONS

Interpreting Degradation of Aging Effects during Liquefaction

Figure 15 compares the relationships between the dynamic small strain shear moduli, G_d, and the effective stress parameter, $(\sigma'_v\cdot\sigma'_h)^{0.5}$ during liquefaction test of the FSs and the RSs. In order to simplify the relationships in Fig. 15, the G_d values measured only at isotropic stress states were plotted for the FSs while all the data were plotted for the RSs, because the G_d values were measured at a large number of points for the FSs in comparison with the RSs as shown in Figs. 5 and 6.

As shown in Fig. 15(a), in the case of Tone-river sand, the G_d value of the FS which was measured at the beginning of liquefaction test was larger than that of the RS. The G_d values of the FSs approached those of the RS when the $(\sigma'_v\cdot\sigma'_h)^{0.5}$ value was approximately 40 to 80 kPa at $\varepsilon_{v(DA)}=1.0\%$ on average. On the other hand, although the G_d values of Edo-river B sand also decreased with the decrease in the effective stress as shown in Fig. 15(b), the

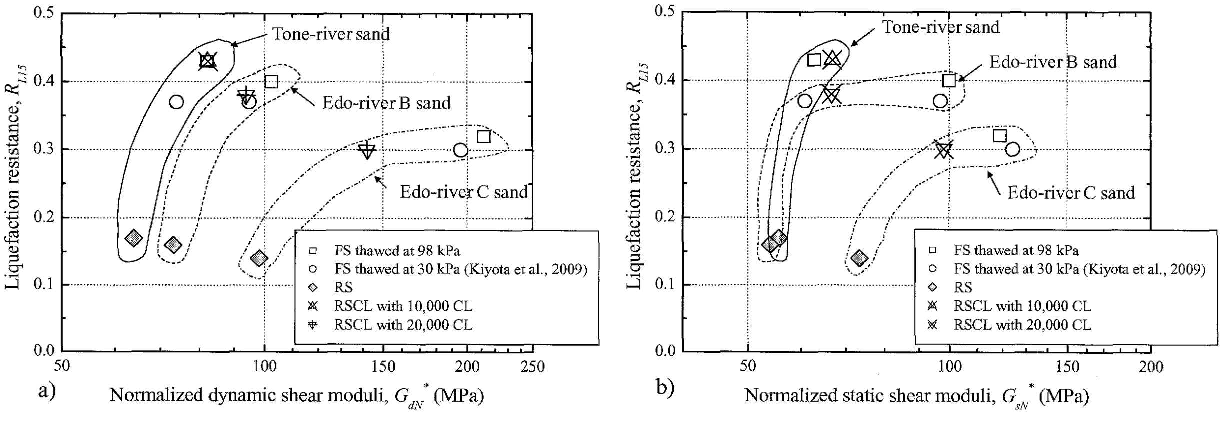

Fig. 14. Relationships between liquefaction resistance and a) G_{dN} and b) G_{sN}^*

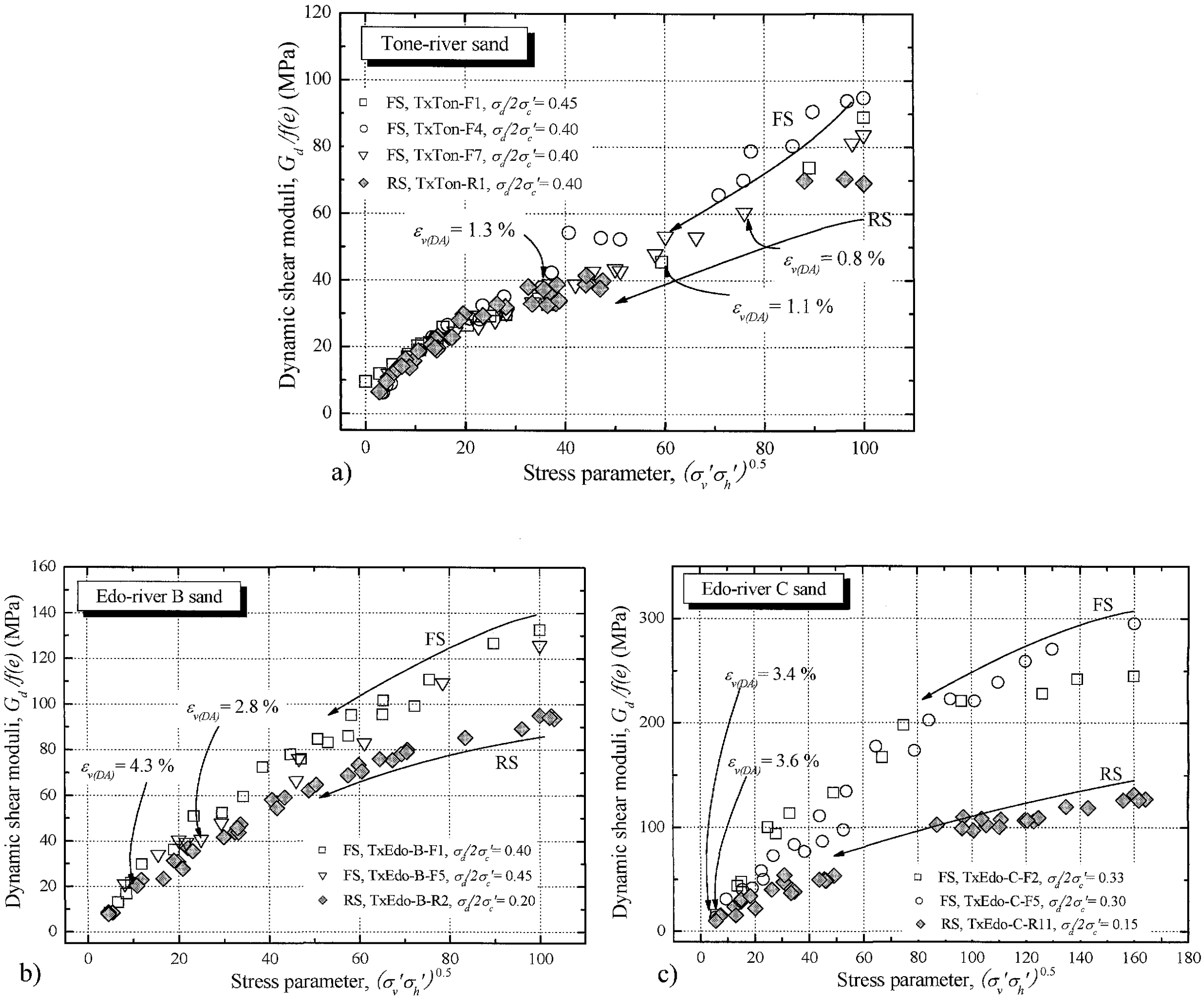

Fig. 15. Comparison of $G_d/f(e)$ during liquefaction between FS and RS on a) Tone-river sand, b) Edo-river B sand and c) Edo-river C sand

Table 3. Summary of applicability of reconstituted sample (RSCL) for in-situ frozen sample (FS)

Sample	Type	States when the aging effects were degraded		Similarity between FS and RSCL	Similarity between FS and RSCL	Applicability of RSCL
		$(\sigma_v'\cdot\sigma_h')^{0.5}$ (kPa)	$\varepsilon_{v(DA)}$ (%)	$N_c/N_{c(3\%)}$-$\varepsilon_{v(DA)}$	$N_c/N_{c(3\%)}$-$\Delta u/\sigma_c'$	
Tone-river	FS	38–76	0.8–1.3	Marginal	Yes	Yes
	$RSCL_{(10000)}$	52–66	0.4–0.6			
Edo-river B	FS	10–25	2.8–4.3	Marginal	No	No
	$RSCL_{(20000)}$	85	0.3			
Edo-river C	FS	5	3.4–3.6	No	No	No
	$RSCL_{(20000)}$	80–115	1.5#			

#: Except for the data with $\varepsilon_{v(DA)}=7.6\%$ in Fig. 15(c)

reduction of the G_d values was slower in comparison with those of Tone-river sand. Moreover, the reduction in the G_d values of Edo-river C sand was slower than that of the Edo-river B sand as shown in Fig. 15(c). In this study, the values of $(\sigma_v'\cdot\sigma_h')^{0.5}$ and $\varepsilon_{v(DA)}$, at which the G_d values of the FSs approached to those of the RSs, are considered as the states when the aging effects of the FSs were completely degraded, and they are summarized in Table 3. However, it is still difficult to evaluate separately the effects of inter-locking and cementation on the liquefaction behaviour.

Consequently, the soil structure of the FSs of Tone-river sand which possibly have only the inter-locking effect would be fragile against generation of excess pore water pressure caused by liquefaction, whereas it would not break easily for the FSs of Edo-river B and C sands

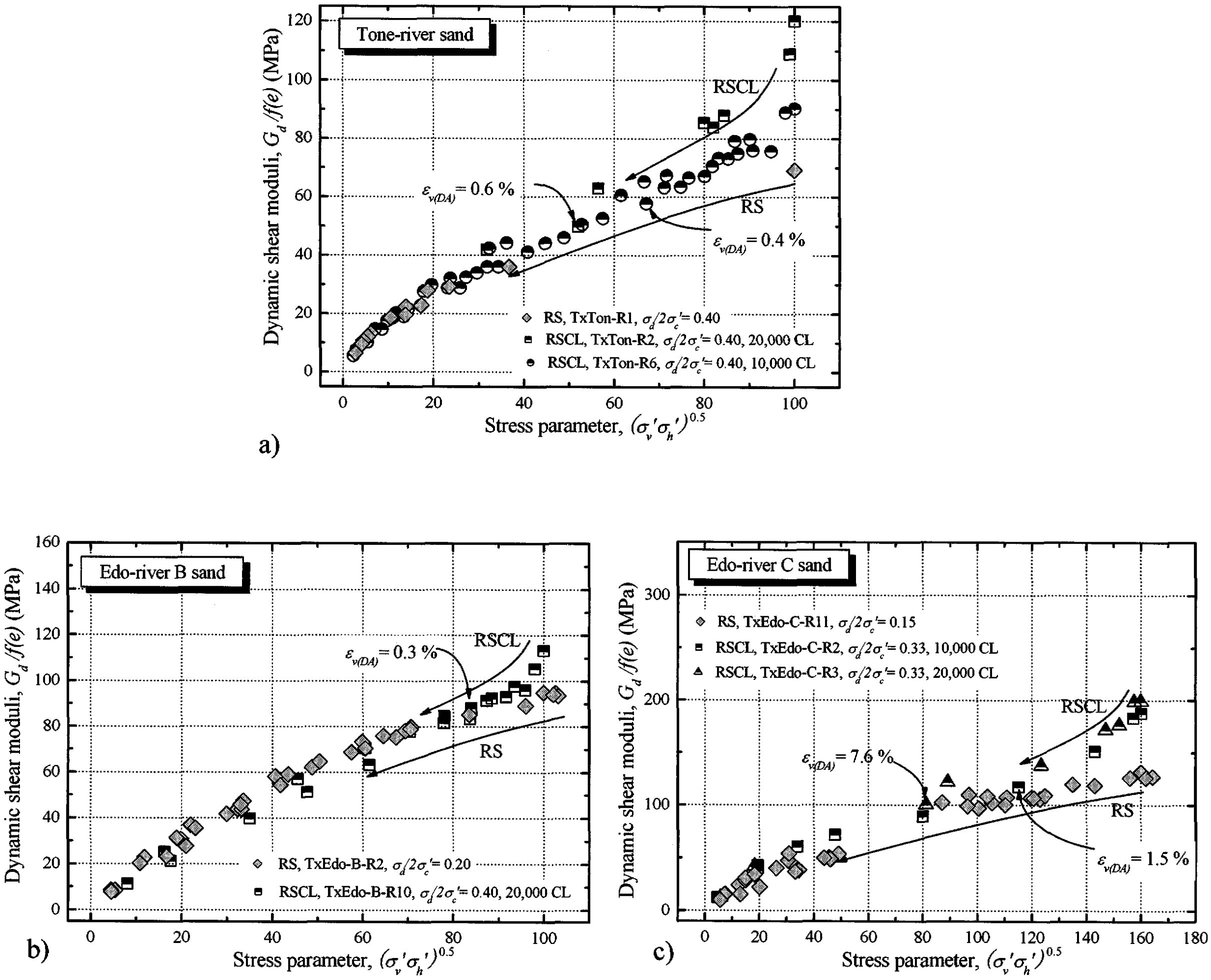

Fig. 16. Comparison of $G_d/f(e)$ during liquefaction between RS and RSCL on a) Tone-river sand, b) Edo-river B sand and c) Edo-river C sand

due to their stronger aging effects; more stable inter-locking and cementation effects. This feature may suggest the fact that liquefaction of Pleistocene deposits has been seldom observed.

Comparisons of the G_d values during liquefaction process between the RSs and the RSCLs are made in Fig. 16. Note again that the G_d values measured only at isotropic stress states were plotted for the RSCLs while all the data were plotted for the RSs. Although the G_d value of RSCLs which was measured at the beginning of liquefaction test was larger than that of the RS, a sudden reduction in the G_d values of RSCLs was observed at an initial part of the liquefaction process. This feature could be seen with all the samples. The values of $(\sigma_v' \cdot \sigma_h')^{0.5}$ and $\varepsilon_{v(DA)}$ at which the G_d values of the RSCLs approached the results of the RSs are shown in Table 3. In the case of the RSCLs, since the increase in the G_d values and liquefaction resistance were due only to inter-locking between soil particles as mentioned previously, the above tendencies of degradation of the G_d values during liquefaction tests corresponded well to those of the FSs of Tone-river sand as shown in Fig. 15(a) and Table 3.

Applicability of Reconstituted Sample for In-situ Frozen Sample

As mentioned previously, good correlations of liquefaction resistance, R_{L15} with dynamic shear moduli, G_d, were obtained for each sample. Tokimatsu et al. (1986) showed similar results by using sands obtained by in-situ freezing and tube samplings. They concluded that it would be a promising means for assessing liquefaction characteristics to measure G_d in the field, to obtain samples by an economical method, and to prestress them to recreate the in-situ shear modulus and density under simulated in-situ stress condition. Therefore, in this study, in order to investigate the applicability of the RSCL in substitution for the FS obtained from Holocene and Pleistocene deposits, the liquefaction behaviour of the RSCL and the FS of each sample were compared in terms of changes in double amplitude vertical strain, excess pore water pressure, and small strain shear moduli.

Figure 17 shows the relationship between the $\varepsilon_{v(DA)}$, and the normalized number of cycles, $N_c/N_{c(3\%)}$, where $N_{c(3\%)}$ is defined as the number of cycles to cause $\varepsilon_{v(DA)}=3\%$. Although the increments in the $\varepsilon_{v(DA)}$ values of the RSCLs were small at an initial part of liquefaction, they were suddenly increased when the $N_c/N_{c(3\%)}$ were about 0.4, 0.7 and 0.9 for Tone-river, Edo-river B and C sands, respectively. On the other hand, the increments in the $\varepsilon_{v(DA)}$ values of FSs were gradual from the beginning to the end of liquefaction. The differences in the above increments between the RSCL and the FS of Edo-river B and C sands were larger than those of Tone-river sand.

Figure 18 shows the relationships between the ratio of excess pore water pressure to the initial confining pressure, $\Delta u/\sigma_c'$, and $N_c/N_{c(3\%)}$. The value of Δu was defined as its minimum value at the respective cycle. In the case of Tone-river sand, the $\Delta u/\sigma_c'$ value of the FS increased gradually with increase in the $N_c/N_{c(3\%)}$, and similar tendencies were obtained with the RSCLs as shown in Fig. 18(a). On the other hand, in the case of Edo-river B and C sands, significant differences were observed between the FSs and the RSCLs as shown in Figs. 18(b) and (c). The fact that both the $\varepsilon_{v(DA)}$ and the $\Delta u/\sigma_c'$ values of FSs are larger than those of RSCLs at the same $N_c/N_{c(3\%)}$ could imply that the persistency of the FSs against liquefaction was stronger than that of the RSCLs in particular with the cases of Edo-river B and C sands.

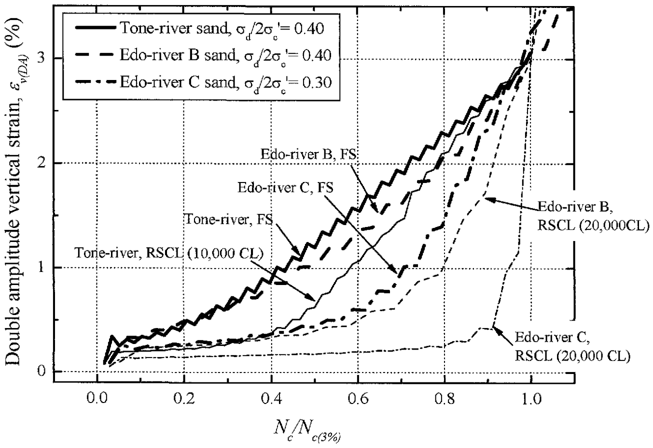

Fig. 17. Relationships between $\varepsilon_{v(DA)}$ and $N_c/N_{c(3\%)}$

Figure 19 shows the G_d values of the FSs and RSCLs of all samples during undrained cyclic triaxial tests, which were measured under the isotropic stress state, plotted versus $(\sigma_v' \cdot \sigma_h')^{0.5}$. Note that the G_d value was normalized by the void ratio function, $f(e)$, in Eq. (6). Decreases in the G_d values during liquefaction were observed with the reduction of the effective stress level on all the specimens. In the case of Tone-river sand, the change in the G_d values of the RSCL seems to correspond to those of the FSs as shown in Fig. 19(a). On the other hand, in the case of Edo-river B and C sands, although a sudden reduction of the G_d values was observed at an initial part of the liq-

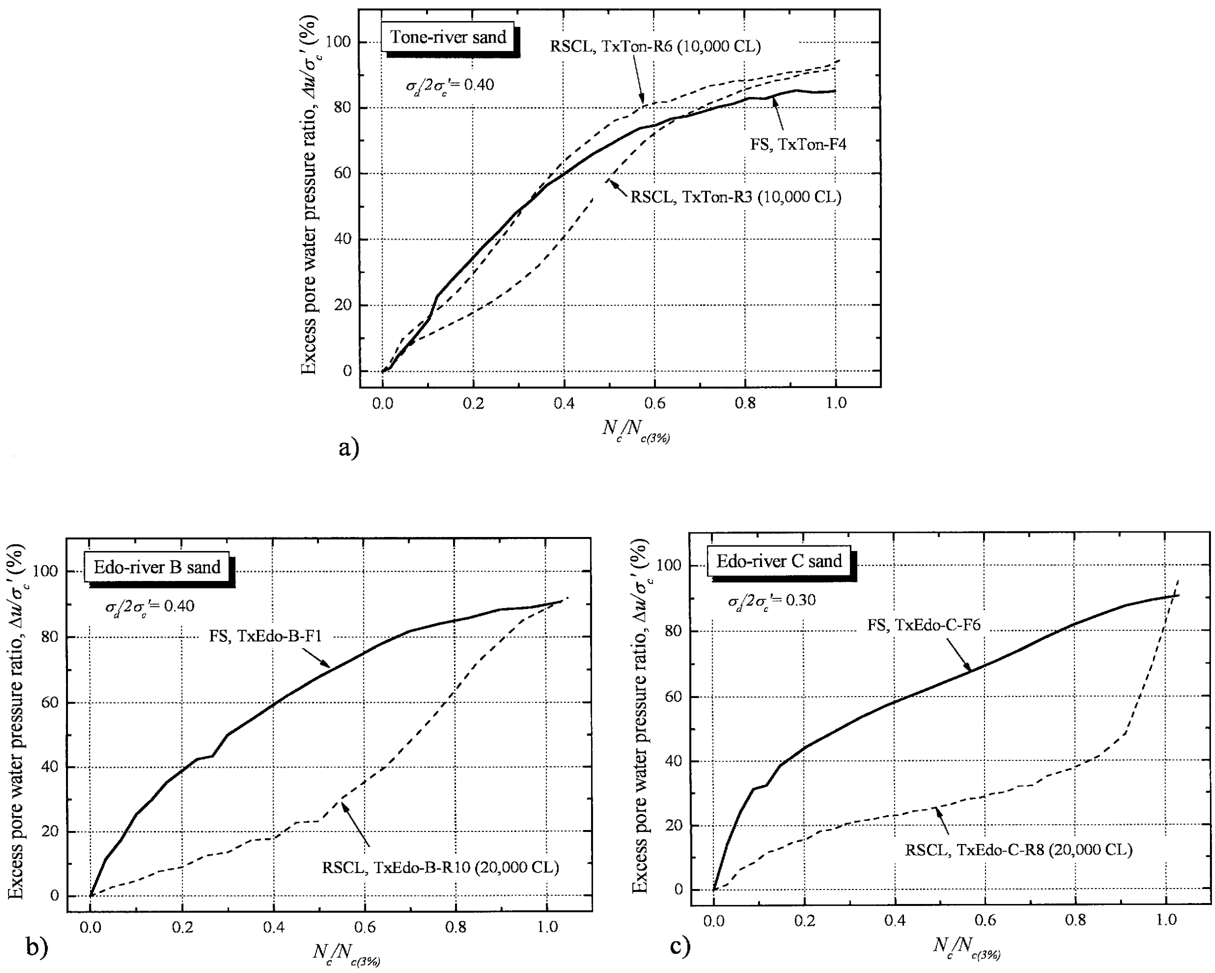

Fig. 18. Comparison of $\Delta u/\sigma_c'$ during liquefaction between FS and RSCL on a) Tone-river sand, b) Edo-river B sand and c) Edo-river C sand

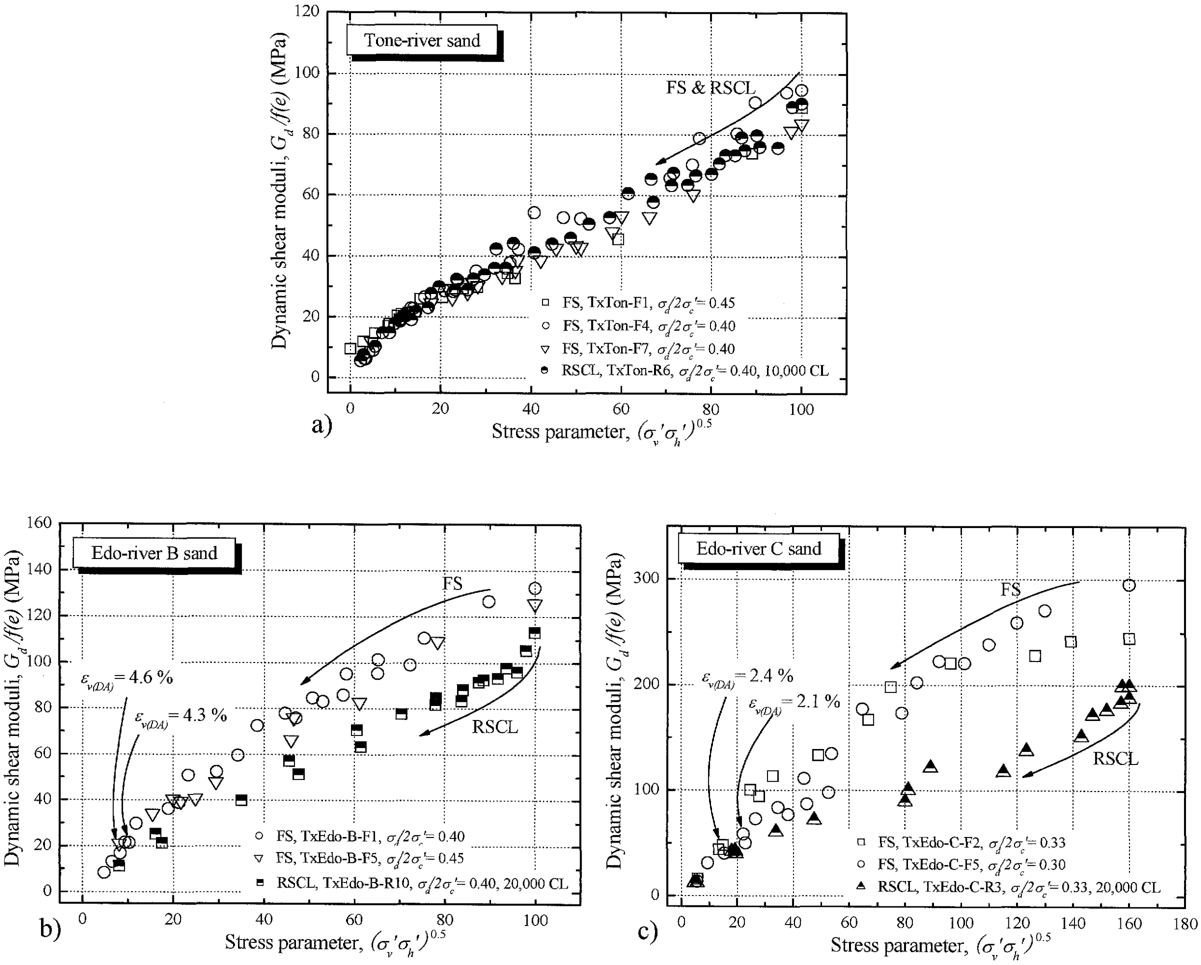

Fig. 19. Comparison of $G_d/f(e)$ during liquefaction between FS and RSCL on a) Tone-river sand, b) Edo-river B sand and c) Edo-river C sand

uefaction process on the RSCL, a slower reduction of the G_d values was observed during liquefaction with the FSs as shown in Figs. 19(b) and (c).

The above contrastive tendencies between Holocene and Pleistocene sands are summarized in Table 3. It would be difficult to simulate the behaviour of the FS which have a cementation effect; i.e., Edo-river B and C sands from Pleistocene deposit, by employing the RSCL even if the G_d values were adjusted by applying drained cyclic loading history. Meanwhile, it would be possible to employ the RSCL in substitution for the FS in the case of un-cemented sample; i.e., Tone-river sand from Holocene deposit.

CONCLUSION

The present paper investigates the effects of aging on small strain shear moduli and liquefaction properties of three kinds of in-situ frozen samples which were retrieved from Holocene (Tone-river sand) and Pleistocene (Edo-river B and C sands) deposits and their reconstituted samples with/without drained cyclic loading history. The conclusions could be summarized as follows;

a) Small strain shear moduli could reflect the extent of natural aging effects of tested samples. Higher values of small strain shear moduli were obtained with the in-situ frozen samples than with the reconstituted samples during isotropic consolidation, and larger difference between them was observed with the Edo-river B and C Pleistocene sands than with the Tone-river Holocene sand. In addition, the small strain shear moduli of the reconstituted samples increased due to drained cyclic loading history.

b) Although the relationships between the liquefaction resistance and the small strain shear moduli which were measured immediately before liquefaction test were not unique among different samples, larger liquefaction resistance was observed with an increase in the small strain shear moduli.

c) From the observation of change in the small strain shear moduli during liquefaction, degradation of the aging effects of the tested samples could be recognized. The soil structure of the Tone-river Holocene sand which have only inter-locking effect would be fragile against the generation of excess pore water pressure, whereas it would not break easily for the Edo-river B and C Pleistocene sands due to more stable inter-locking and cementation effects.

d) During the liquefaction process of the Tone-river

Holocene sand, similar tendencies of changes in the double amplitude vertical strain, excess pore water pressure and small strain shear moduli could be observed between the in-situ frozen sample and their reconstituted sample which has drained cyclic loading history. On the other hand, the above tendencies were different between the in-situ frozen sample and their reconstituted sample for the Edo-river B and C Pleistocene sands. Consequently, the application of the reconstituted sample in substitution for in-situ frozen sample, as suggested by Tokimatsu and Hosaka (1986) for assessing in-situ liquefaction characteristics, would be relevant in the case of less-cemented sample, whereas it seems difficult to simulate fully the liquefaction behaviour of in-situ frozen sample which has higher cementation effect.

ACKNOWLEDGEMENTS

The in-situ frozen samples and the relevant in-situ survey data were provided by the courtesy of Incorporated Administrative Agency Public Works Research Institute, Japan.

REFERENCES

1) AnhDan, L. and Koseki, J. (2003): Anisotropic deformation properties of dense granular soils by large-scale true triaxial tests, *Deformation Characteristics of Geomaterials* (eds. by Di Benedetto et al.), Swets & Zeitlinger, Lisse, 305–312.
2) Barton, M. E. (1993): Cohesive sands: The natural transition from sands to sandstones, *Geotechnical Engineering of Hard Soils-Soft Rocks* (eds. by Anagnostopoulos et al.), Balkema, 367–374.
3) Drnevich, V. P. and Richart, F. E. (1970): Dynamic prestraining of dry sand, *Journal of Soil Mechanics Foundation Division*, ASCE, **96**(SM2), 453–467.
4) Goto, S. (1986): Strength and characteristics of granular materials in triaxial tests, *Dr. of Eng. Thesis*, Univ. of Tokyo.
5) Goto, S. (1993): Influence of a freeze and thaw cycle on liquefaction resistance of sandy soils, *Soils and Foundations*, **33**(4), 148–158.
6) Goto, S., Tatsuoka, F., Shibuya, S., Kim, Y. S. and Sato, T. (1991): A simple gauge for local small strain measurement in the laboratory, *Soils and Foundations*, **31**(1), 169–180.
7) Goto, S., Suzuki, Y., Nishio, S. and Oh-oka, H. (1992): Mechanical properties of undisturbed Tone-river gravel obtained by in-situ freezing method, *Soils and Foundations*, **32**(3), 15–25.
8) Goto, S., Matsueda, S., Morii, Y. and Sueoka, T. (1999): Small strain stiffness of sands in isotropic compression and liquefaction tests, *Pre-failure Deformation Characteristics of Geomaterials*, Balkema, Rotterdam, 275–281.
9) Hardin, B. O. and Richart, F.E. (1963): Elastic wave velocities of granular soils, *Journal of ASCE*, **89**(1), 33–65.
10) Hatanaka, M., Sugimoto, M. and Suzuki, Y. (1985): Liquefaction resistance of two alluvial volcanic soils sampled by in situ freezing, *Soils and Foundations*, **25**(3), 49–63.
11) Hoque, E. and Tatsuoka, F. (1998): Anisotropy in elastic deformation of granular materials, *Soils and Foundations*, **38**(1), 163–179.
12) Kiyota, T., Koseki, J., Sato, T. and Tsutsumi, Y. (2009): Effects of sample disturbance on small strain characteristics and liquefaction properties of Holocene and Pleistocene sandy soils, *Soils and Foundations* (accepted conditionally for possible publication).
13) Koseki, J., Kawakami, S., Nagayama, H. and Sato, T. (2000): Change of small strain quasi-elastic deformation properties during undrained cyclic torsional shear and triaxial tests of Toyoura sand, *Soils and Foundations*, **40**(3), 101–110.
14) Koseki, J. and Ohta, A. (2001): Effects of different consolidation conditions on liquefaction resistance and small strain quasi-elastic deformation properties of sands containing fines, *Soils and Foundations*, **41**(6), 53–62.
15) Seed, H. B. (1979): Soil liquefaction and cyclic mobility evaluation for level ground during earthquakes, *Journal of the Geotechnical Engineering Division*, ASCE, **105**(GT2), 201–255.
16) Tanaka, Y., Kudo, K., Nishi, K. and Okamoto, T. (1994): Shear modulus and damping ratio of gravelly soils measured by several methods, *Pre-failure Deformation of Geomaterials*, Balkema, 47–53.
17) Tanizawa, S., Teachavorasinskun, S., Yamaguchi, J., Sueoka, T. and Goto, S. (1994): Measurement of shear wave velocity of sand before liquefaction and during cyclic mobility, *Pre-failure Deformation of Geomaterials*, Balkema, Rotterdam, 63–68.
18) Tatsuoka, F. and Kohata, Y. (1995): Stiffness of hard soils and soft rocks in engineering applications, *Pre-failure Deformation of Geomaterials* (eds. by Shibuya et al.), Balkema, 947–1063.
19) Tatsuoka, F., Jardine, R. J., Lo Presti, D., Di Benedetto, H. and Kodaka, T. (1997): Characterising the pre-failure deformation properties of geomaterials, *Theme lecture of 14th ICSMFE*, **4**, 2129–2164.
20) Tatauoka, F., Ishihara, M., Uchimura, T. and Gomes Correia, A. (1999): Non-linear resilient behaviour of unbound granular materials predicted by the cross-anisotropic hypo-quasi-elasticity model, *Proc. Workshop on Modelling and Advanced testing for Unbound Granular Materials* (ed. by Correia), Lisboa, Balkema, 197–204.
21) Teachavorasinskun, S., Tatsuoka, F. and Lo Presti, D. C. F. (1994): Effects of the cyclic prestraining on dilatancy characteristics and liquefaction strength of sand, *Pre-failure Deformation of Geomaterials*, Balkema, Rotterdam, 75–80.
22) Tokimatsu, K. and Hosaka, Y. (1986): Effects of sample disturbance on dynamic properties of sand, *Soils and Foundations*, **26**(1), 53–64.
23) Tokimatsu, K., Yamazaki, T. and Yoshimi, Y. (1986): Soil liquefaction evaluations by elastic shear moduli, *Soils and Foundations*, **26**(1), 25–35.
24) Tokimatsu, K. and Uchida, A. (1990): Correlation between liquefaction resistance and shear wave velocity, *Soils and Foundations*, **30**(2), 33–42.
25) Wichtmann, T. and Triantafyllidis, T. (2004): Influence of a cyclic and dynamic loading history on dynamic properties of dry sand, part II: cyclic axial preloading, *Soil Dynamics and Earthquake Engineering*, **24**, 789–803.
26) Yamashita, S., Hori, T. and Suzuki, T. (2003): Effects of fabric anisotropy and stress condition on small strain stiffness of sands, *Proc. International Workshop on the Deformation Characteristics of Geomaterials*, 187–194.
27) Yoshida, N., Goto, H., Aoi, S., Fukumoto, S. and Mikami, T. (2007): Investigation on record at K-NET Kashiwazaki during the 2007 Niigataken-chuetsu-oki earthquake, http://www.civil.tohoku-gakuin.ac.jp/yoshida/inform/chuetsuoki/k-net-e.pdf.
28) Yoshimi, Y., Tokimatsu, K., Kaneko, O. and Makihara, Y. (1984): Undrained cyclic shear strength of a dense Niigata sand, *Soils and Foundations*, **24**(4), 131–145.
29) Yoshimi, Y., Tokimatsu, K. and Ohara, J. (1994): In situ liquefaction resistance of clean sands over a wide density range, *Geotechnique*, **44**(3), 479–494.
30) Zhou, Y. and Chen, Y. (2005): Influence of seismic cyclic loading history on small strain shear modulus of saturated sands, *Soil Dynamics and Earthquake Engineering*, **25**, 341–353.